Higher Order Output Filter Design for Grid Connected Power Converters

Parikshith.B.C, Dr.Vinod John
Department of Electrical Engineering
Indian Institute of Science
Bangalore, Karnataka, India 560012
Email: pariks@ee.iisc.ernet.in

Abstract—Design of higher order LCL filters that are used in grid-connected inverter applications involves multiple constraints. The filter requirements are driven by tight filtering tolerances of standards such as IEEE 519-1992 and IEEE P1547.2-2003. Higher order LCL filters are essential to achieve these regulatory standard requirements at compact size and weight. This paper discusses the design procedure for these higher order LCL filters. The design procedure is analysed in per-unit basis so results can be generalized for different applications and power levels. This paper also gives guidelines for actual construction of the inductor based on a proposed fringing flux model. Experimental results of filtering characteristics show a good match with analysis in the frequency range of interconnected inverter applications.

Keywords: current ripple, ferrite core, fringing effect, LCL filter, per unit, transfer function.

I. INTRODUCTION

Active Front End converters are used to improve power quality of drives and electronic loads at the point of common coupling to the grid. The conventional method to interface these converters to the grid is through a simple first order low-pass filter ie L filter. But such a filter is bulky, inefficient and cannot meet the regulatory requirements regarding interconnection of harmonic loads to grid [1]- [2]. This paper discusses the design procedure for higher order filters (LC, LCL) for medium to high power three phase converters. The design calculations are based on per-unit values, so the results obtained are generalized for medium power levels of 10 to 100's of kW. The volt-ampere rating of the power converter is the base KVA. The fundamental frequency single-phase line to neutral voltage of the converter is V_{base}.

$$I_{base} = \frac{KVA_{base}}{3 \times V_{base}} \tag{1}$$

$$Z_{base} = \frac{V_{base}}{I_{base}} \tag{2}$$

Some assumptions are made to simplify the initial analysis: All filter elements are considered ideal, i.e no winding resistance, inter-turn/inter-winding capacitance in case of inductor, and no equivalent series resistance or parasitic inductance in case of capacitor. Grid is considered as an ideal voltage source, i.e having zero impedance, and supplying constant voltage/current at fundamental (50Hz) frequency. The system configuration assumed for further analysis is given in Fig 1.
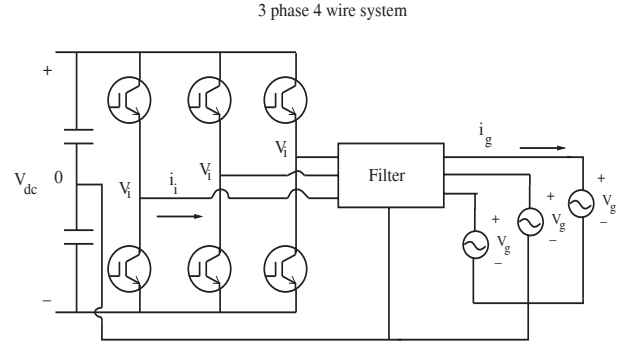
3 phase 4 wire system

Fig. 1.   Three phase four wire system with neutral grounding

Section II discusses the transfer function analysis method which is the basis for design of higher order filters. All filter types starting from first order L filter upto third order LCL filter are discussed and compared. Section III focuses on actual construction details of the inductor. A new simple empirical reluctance model which takes into account the fringing of magnetic flux at large air gaps is introduced. In Section IV preliminary experimental results are discussed.

II. TRANSFER FUNCTION ANALYSIS

The inductive part of the low pass filter is designed based on the allowable current ripple at switching frequency on the grid side. On a per-unit basis, the inductance is

$$L_{pu} = \frac{V_{dc(pu)} \times D \times (1-D) \times \pi}{f_{sw(pu)} \times \sqrt{3} \times \delta i_{g(pu)}} \tag{3}$$

where D is the duty ratio, assuming sine-triangle modulation, $V_{dc(pu)}$ is the dc bus voltage and $\delta i_{g(pu)}$ is the rms value of the switching frequency ripple current on the grid side. The ripple current on the grid side that can be injected by any power converter is specified by the IEEE standard 519-1992. For example, the IEEE 519 recommended maximum current distortion for a $I_{SC}/I_L < 20$ for current harmonics $\geq 35^{th}$ is 0.3%. I_{SC} refers to short circuit current and I_L is the nominal load current. This requirement of 0.3% refers to a "weak" grid. The percentage of ripple current can be higher for a "stiff" grid [2]. Since most inverters can switch at higher frequencies exceeding 2 kHz using current IGBT technology, the standard refers to harmonics $\geq 35^{th}$.

A. LC filter

The output voltage of a grid connected power converter cannot be controlled since it is decided by the grid conditions. The filter input current i_i is usually sensed and given back as feedback to close the control loop. But the grid current i_g is the control variable which is controlled by varying the inverter pole voltage. Hence, the transfer function which decides the closed loop performance of the filter is the transfer function between output current and input voltage of the filter for zero grid voltage.
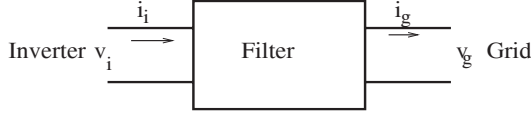

Fig. 2. Filter per phase block diagram

The transfer function of grid current i_g to inverter voltage v_i is same for L and LC filters when parasitic grid impedences are neglected (Fig 3). Therefore, the size of inductor does not change from L to LC filter. The parasitic grid inductance tends to increase the order of the LC filter.

$$\left|\frac{i_g(s)}{v_i(s)}\right|_{v_g \ short} = \frac{1}{sL} \tag{4}$$
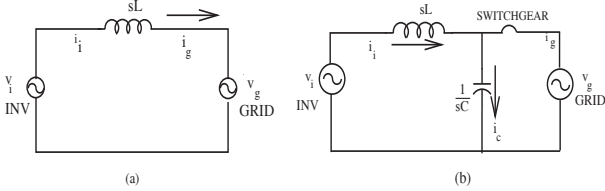

Fig. 3. (a)L filter between inverter and grid; (b)LC filter between inverter and grid; v_i and i_i are the inverter voltage and current per phase and v_g and i_g are the grid voltage and current per phase. i_c is the capacitor current per phase.

B. Bandwidth consideration and Capacitor Selection

The capacitance of the LC filter is decided by the resonant frequency. In turn the resonant frequency depends on the bandwidth of the closed loop system. Since the bandwidth of the closed loop system is decided by the filter elements and the control algorithm, it cannot be used straightaway in the design process. Here, we estimate the maximum possible system bandwidth and use it in our design procedure. The maximum possible bandwidth is certainly not achieved in practice, but this assumption is reasonable for a first pass iteration. Figure 4 shows the closed loop system.

Assuming the controller acts directly at the modulator without prior dynamics, there are two delays in the closed loop system which limit the bandwidth.

1) The Inverter response delay. When the voltage command to the inverter is changed, in the worst case, it takes $T_{sw}/2$ time for the voltage output of the inverter to change, where T_{sw} is the switching time period.

2) Current sampling and computational delay. If the current sampling is sampled once per pwm cycle this delay would be T_{sw}. Here we are assuming that the current is sampled twice every cycle, on the rising half and falling half of the PWM switching signal, so the delay in sensing is $T_{sw}/2$.
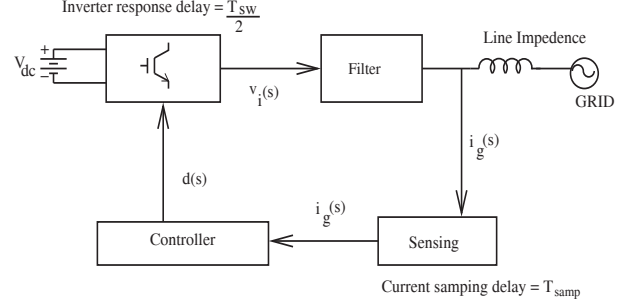

Fig. 4. Closed loop system bandwidth assuming no delay in controller

So the total system excluding the filter is essentially modelled as a pure delay e^{-st_d}, where is $t_d = T_{sw}$. The resonant frequency is placed such that the closed loop system including the LC filter gives a phase margin of atleast $45°$. The LC filter transfer function which affects the closed loop system bandwidth is:

$$\frac{i_g(s)}{v_i(s)} = \frac{1}{sL} \tag{5}$$

Since the LC filter transfer function has a constant phase of -$90°$ for all frequencies, the bandwidth of the system(excluding the filter) is limited at the frequency where its phase is $45°$. So the frequency at which the phase margin of the total system (LC filter + delay) is $45°$ can be calculated.

$$\omega_{bw} = \frac{45° \dfrac{\pi}{180°}}{t_d} \tag{6}$$

Now the resonant frequency can be placed with reference to the bandwidth. If the resonant frequency is within the bandwidth of the closed loop system, active damping methods can be used to attenuate the filter resonance peaks. If the resonant frequency is outside the bandwidth of the system, passive damping methods (i.e resistors) must be used. Active damping means lower power loss at full load. Passive damping is essential in grid connected applications, in case the inverter is switched off while still being connected to the grid.

$$C_{pu} = \frac{1}{f_{res(pu)}^2 \times L_{pu}} \tag{7}$$

Eq (4) will change if LC filter is connected to a stand-alone load. Consider an LC filter connected between an inverter and external load of $R=1$ pu resistance. Then the transimpedance transfer function will be

$$\frac{i_g}{v_i} = \frac{1}{s^2 LCR + sL + R} \tag{8}$$

C. LCL filter

An LCL filter is preferred to an L filter in high power and/or low switching frequency applications. This is because of the higher order of the LCL filter means the higher roll-off of 60dB/decade for the same (or lower) net inductance (i.e $L_1 + L_2$).
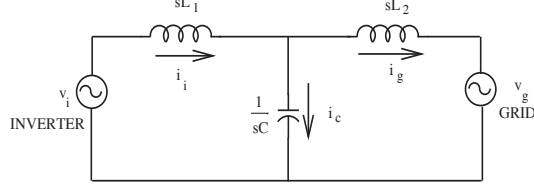

Fig. 5.   LCL filter inserted between front end converter and grid

The procedure for design of LCL filter given in the current literature is as follows [3]– [6].

- L_1 is designed based on the current ripple.
- L_2 is assumed to be a fraction of L_1, maybe greater than or lesser than L_1. This is decided by the current ripple in inductor L_2.
- C is designed on the basis of the reactive power supplied by the capacitor at fundamental frequency.

This procedure has a few limitations.

- It is not possible to design the LCL filter on a per unit basis, where the per unit is referenced from the VA of the system
- The resonant frequencies and their effect on system bandwidth is ignored in this method.
- Even though the aim of filter design is to attenuate the switching frequency harmonics, the basis of capacitor design is the reactive power of fundamental frequency.
- There is no simple way to compare L and LCL filters for the same application.

In our proposed method the inverter plus filter is treated as a "black box," so the only input variables for the filter design are the KVA rating of the inverter and the switching frequency output current ripple $i_g(j\omega_{sw})$. Let L be the *total* inductance of the filter,

$$L = L_1 + L_2 \tag{9}$$

The relation between L_1 and L_2 is

$$L_1 = a_L L_2 \tag{10}$$

Next, the total system bandwidth (including filter) is estimated such that there is acceptable phase margin in the system. The LCL filter transfer function which affects the closed loop system bandwidth in grid connected mode of operation is

$$\frac{i_g(s)}{v_i(s)} = \frac{1}{s^3 L_1 L_2 C + s(L_1 + L_2)} \tag{11}$$

The LCL filter transfer function has a constant phase of -90° below ω_{res} and +90° above ω_{res} as can be seen from Eq (11). So the bandwidth of the closed loop system will be same as that of the LC filter below ω_{res}. The resonant frequency of

interest is $\omega_{L_p C}$, since this is the resonant frequency of Eq (11).

$$\omega_{res}^2 = \frac{1}{L_p C} \tag{12}$$

where

$$L_p = \frac{L_1 \times L_2}{L_1 + L_2} \tag{13}$$

Substituting for L_p in terms of $L = L_1 + L_2$ and converting all quantities to their per-unit equivalents, the resonant frequency is

$$\omega_{res(pu)}^2 = \frac{1}{C_{pu} \times L_{pu} \dfrac{a_L}{(a_L + 1)^2}} \tag{14}$$

The capacitance in an LCL filter depends on the resonant frequency ω_{res} and the ratio in which we distribute the total inductance $L_1 + L_2$. Assuming we have fixed ω_{res}, the ratio of L_1 and L_2 for minimum capacitance is given by

$$\frac{\delta C_{pu}}{\delta a_L} = 0 \tag{15}$$

which simplifies to $a_L = 1$. So the smallest capacitance value of LCL filter is obtained when $L_1 = L_2$. Eq (12) becomes

$$\omega_{res}^2 = \frac{4}{L_{pu} C_{pu}} \tag{16}$$

To find L_{pu} and C_{pu}, Eq (11) is evaluated (in per unit) at switching frequency f_{sw}.

$$\left| \frac{i_g(j\omega_{sw})}{v_i(j\omega_{sw})} \right| = \frac{1}{|-j\omega_{sw}^3 L_1 L_2 C + j\omega_{sw}(L_1 + L_2)|} \tag{17}$$

$i_g(j\omega_{sw})$ is the switching ripple current at the point of common coupling to the grid at switching frequency. This is guided by the recommendations of IEEE 519-1992 or IEEE P1547.2-2003 standard. $v_i(j\omega_{sw})$ is the inverter pole voltage ripple at switching frequency, which is $V_{dc}/2$.

Eq (17) is solved by converting all parameters to per-unit and substituting Eq (16) in Eq (17).

$$L_{pu} = \frac{1}{\omega_{sw(pu)} \left| \dfrac{i_{g(pu)}}{v_{i(pu)}} \right| \left| 1 - \dfrac{\omega_{sw(pu)}^2}{\omega_{res(pu)}^2} \right|} \tag{18}$$

Then C_{pu} will be calculated from Eq (16). To check the condition that L_{pu} meets the specifications of current ripple, the current ripple δi_L for the total inductance $L_1 + L_2$ is calculated using Eq (3). If the current ripple exceeds the maximum allowed, L_{pu} is multiplied by some factor k to keep the switching current ripple within reasonable limits of 0.1 to 0.2 pu. The resonant frequency is maintained by dividing C_{pu} by the same factor k.

The advantage of this method compared to [3]– [6] is that it simultaneously satisfies four constraints of filter design. The voltage drop across the inductor at fundamental frequency will be less than 0.1 pu (table I). And the reactive current sourced by the capacitor at fundamental frequency will also be less than 0.1 pu. The switching frequency attenuation requirement and bandwidth requirements are already met as discussed above.

TABLE I
COMPARISON OF PU VALUES OF FILTER FOR SAME GRID CURRENT RIPPLE

	L	LC	LCL
Inductance(pu)	2.352	2.352	0.105
Capacitance(pu)	-	1.063×10^{-3}	0.095
$\delta i_{g(pu)}$	0.003	0.003	0.003
$f_{res(pu)}$	-	20	20
$f_{sw(pu)}$	200	200	200

Fig. 6.   Fringing effect approximation from [9]

III. CONSTRUCTION DETAILS

The energy handling capability of an inductor is defined by the area product A_p which is the product of window area A_w and core cross section area A_e [8].

$$A_p = \frac{V_f I_f}{k_f k_u f B_m J_m} \tag{19}$$

where V_f is the voltage across the inductor at frequency f, I_f is the current through the inductor, k_f is the form factor (k_f=4.44 for sinusoidal waves), k_u is the core window utilization factor, B_m is the maximum allowable flux density in the core before saturation and J_m is the current density limit in the conductors to prevent overheating of the winding.

The fundamental current in the inductor I_f can vary depending on the grid side voltage. To ensure that the inductor core does not saturate for the highest current possible, the inductor is oversized by a certain factor. The minimum grid side voltage is assumed to be 90% of the nominal rating. In that case, the maximum inductor current is

$$I_f = \frac{KVA_{base}}{3 \times 0.9 \times V_{base}} \tag{20}$$

Then the voltage across the inductor is

$$V_f = |I_f \times j\, 2\pi f L| \tag{21}$$

The material chosen for the core is Ferrite N 87 manufactured by EPCOS. The flux density is limited to B_m=0.35 T. The current density limit depends on the allowable temperature rise in the inductor. As a first estimate it is chosen arbitrarily to be $J_m = 3 \times 10^6$ A/m². The frequency f is the grid fundamental frequency of 50 Hz.

Once the area product A_p is obtained, the appropriate core size has to be chosen. The next step is to decide on the number of turns and required air gap. The combination of low flux density of ferrite material and high current rating meant that the inductor inevitably will have a large air gap. The fringing of the magnetic flux at the air gap introduces significant errors in the estimated value of inductance. This prompted the search for an accurate and simple air gap reluctance model to account for the fringing effect.

A. Fringing model

This model is a modification of the fringing estimate given by [9]. This model was chosen because of its simplicity and acceptable accuracy. The fringing at the air gap is modeled as increase in area of the air gap cross section, and this increase
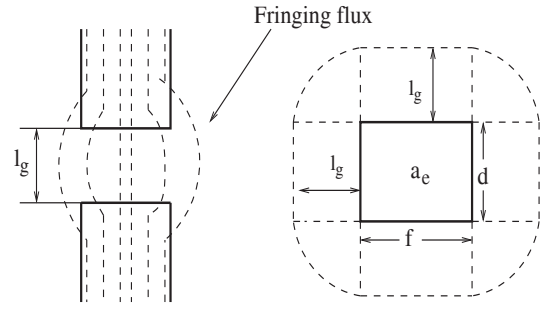
is in terms of l_g. The air gap reluctance $\Re_g$ for an air gap of l_g and core cross section area of $a_e = f \times d$ is given by

$$\Re_g = \frac{l_g}{\mu_0[a_e + (f + d)l_g + l_g^2]} \tag{22}$$

Eq (22) was giving an error of 25% between the theoretical calculated inductance and the actual measured value. The original equation was altered to reflect the actual inductance that was measured. So Eq (22) was modified to

$$\Re_g = \frac{l_g}{\mu_0[a_e + 2(f + d)l_g + \pi l_g^2]} \tag{23}$$
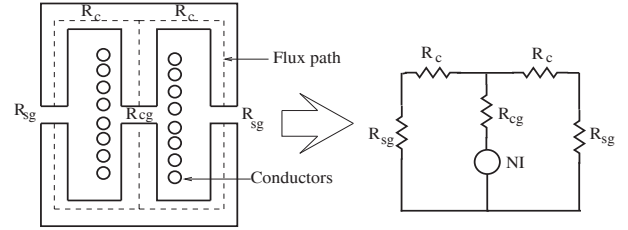
In the case of EE type of core from Fig 7, there are three

Fig. 7.   Magnetic circuit representation of EE core inductor

possible reluctances: reluctance of the core $\Re_c$, reluctance of the center leg of E core $\Re_{cg}$ and reluctance of side leg of E core $\Re_{sg}$. The total reluctance of the magnetic path will be

$$\Re_t = \Re_{cg} + \frac{\Re_{sg}}{2} + \frac{\Re_c}{2} \tag{24}$$

B. Graphical Iterative method

In the design process of an inductor, there are two parameters that must be accurately preserved i.e L and B_m and two parameters that can be modified N and l_g. So L and B_m are basically functions of 2 variables.

$$L = f(N, l_g) \tag{25}$$

$$B_m = g(N, l_g) \tag{26}$$

Using the fringing model stated above, we can define the functions $f(N, l_g)$ and $g(N, l_g)$ as

$$L = \frac{N^2}{\Re_t} \tag{27}$$

TABLE II
FINAL INDUCTOR SPECIFICATIONS FOR LCL FILTER

L_{req}	L_{frg}	I_{rms}	I_p	N	l_g
3.229 mH	3.487 mH	14.58 A	22.4 A	120	12 mm

$$B_m = \frac{N I_p}{A_e \Re_t} \tag{28}$$

I_p is the peak current flowing through the inductor. Since the filter inductor carries both the fundamental current I_f and the switching frequency current I_{sw}, the peak current rating of the inductor I_p is calculated as the sum of the peak fundamental and switching frequency currents. The fundamental current is sinusoidal and the switching frequency current is assumed to be triangular.

$$I_p = I_f \times \sqrt{2} + I_{sw} \times \sqrt{3} \tag{29}$$

Both L and B_m are plotted as functions of (l_g, N). The dark shaded region(or red) in Fig. 8 indicates the values of (l_g, N) for which B_m exceeds the limit of 0.35 T. The unshaded region(or yellow) in Fig. 9 indicate the values of (l_g, N) for which L exceeds the required inductance of 3.2 mH. So for a good design we have to stay outside of the dark shaded region (Fig. 8) and stay as close as possible (or even inside) the unshaded region (Fig. 9). The intersection of these two conditions gives the possible (l_g, N) for which the core will not saturate as well as the required inductance is achieved. This means that a core which passes the Area Product criterion need not necessarily give a feasible design.

The final core chosen is EPCOS UU 93/152/30. The final values of (l_g, N) can be observed in Fig. 10. L (straight line) is in a range of 3.4-3.5 mH, and B_m(dashed line) is in a range of 0.38-0.4 T. The possible values of (l_g, N) which give (L, B_m) in this range are plotted and fit using a third order polynomial function. The intersection of both curves gives the value of (l_g, N). The final inductor specifications are in table II.
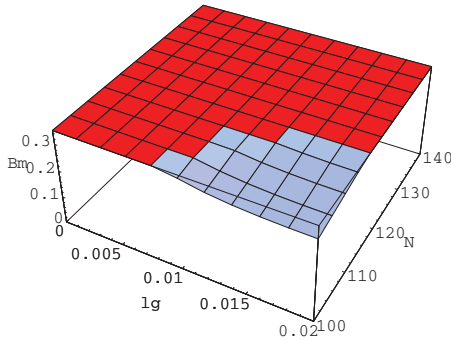

Fig. 9.   Inductance plot of UU 93/152/30 core
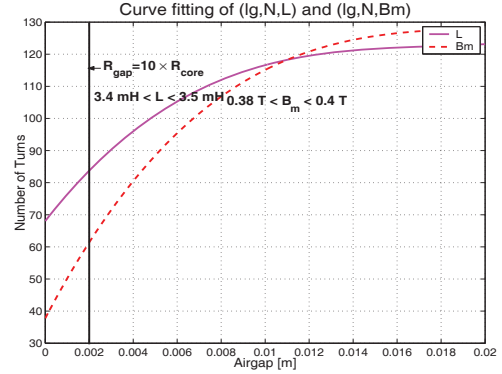
Fig. 10.   Intersection of required inductance and flux density limit

Fig. 8.   Flux density plot of UU 93/152/30 core

IV. EXPERIMENTAL DATA

A. Inductance measurement

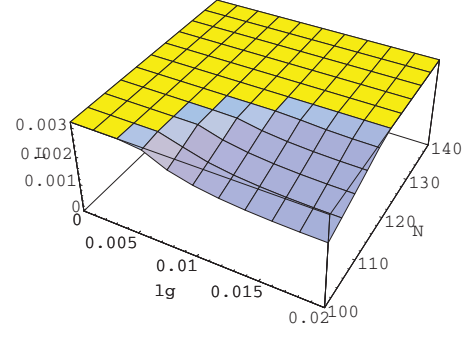Each inductor was supplied with the rated current at fundamental frequency and the voltage drop across the inductor and current through the inductor was measured using a digital power meter. This gave most the accurate measurement of the inductance.

B. Frequency response

The frequency response of the LCL filter was measured using a network analyzer. The applied sinusoidal signal of $1.4V_{p-p}$ was swept from 10 Hz to 100 kHz with 500 frequency values in this range, each value averaged over 20 samples. The transfer functions of i_g/v_i and v_g/v_i are plotted and compared with their theoretical equivalents.

The continuous (blue) line shows the simulated plot assuming ideal filter characteristics. The experimental data is plotted on the dotted (magenta) line. The experimental data shows a double zero at 35 k rad/s. This double zero is because of the resonance between the capacitance C and parasitic inductance L_c in the capacitive branch. This parasitic inductance is due to inductance of the copper leads connecting the capacitor to the two inductances L_1 and L_2. The parasitic inductance was calculated from the frequency response to be 40 μH.

V. CONCLUSION

The method of higher order filter design proposed in this paper achieves the goal of a compact and lightweight filter while meeting the regulatory requirements. The assumptions made for simplified analysis do not significantly alter the
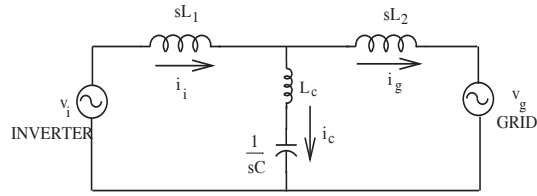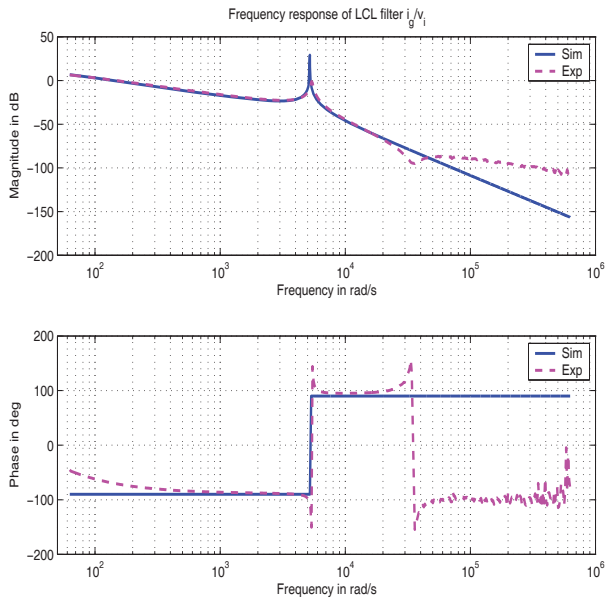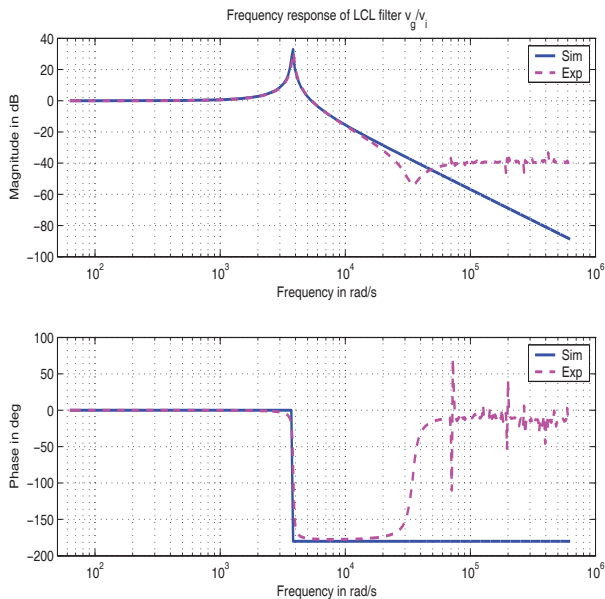
Fig. 11.   Parasitic inductance in capacitance branch

results. The design procedure ensures that the parasitics of the filter components are kept as low as possible. For eg, the winding resistance of inductor and the equivalent series resistance of the capacitor are very low and have no effect on the overall transfer function. Similarly, inter-turn/inter-winding capacitance of the inductor is also very low and has no effect on the frequency response. The effect of parasitic inductance is felt only at frequencies greater than to switching frequency and it can be reduced by proper construction.

The per unit calculation of filter parameters ensures filter design is most general and at the same time allows for easy comparison of filter size of different filter types. The proposed empirical model to account for fringing effect can accurately specify the inductance even with large air gaps. The filtering characteristics of the LCL filter is verified using a network analyzer. Future work will include the constraints of thermal effects on the filter design.

VI. APPENDIX

System ratings:

V_{ph}	KVA	Z_{base}	f_{sw}
254.03 V	10 KVA	19.353 Ω	10 kHz

Filter specifications:

	Required	Actual
L_1	3.229 mH	3.48 mH
L_2	3.229 mH	3.89 mH
C	15.69 μF	20 μF

Fig. 12.   Frequency response of LCL filter i_g/v_i

Fig. 13.   Frequency response of LCL filter v_g/v_i

REFERENCES

[1] "IEEE P1547.2 Draft Application Guide for IEEE 1547 Standard for Interconnecting Distributed Resources with Electric Power Systems," IEEE P1547.2-2003
[2] "IEEE Recommended Practices and Requirements for Harmonic Control in Electrical Power Systems," IEEE 519-1992
[3] M.Liserre, F.Blaabjerg and A. Dell'Aquila, "Step-by-step design procedure for a grid-connected three-phase PWM voltage source converter," *Int. J. Electronics*,vol. 91, no. 8, pp. 445-460, Aug 2004.
[4] Y.Lang, D.Xu, et al., "A novel design method of LCL type utility interface for three-phase voltage source rectifier," *IEEE 36th Conference on Power Electronics Specialists, 2005.*
[5] B.Bolsens, K. De Brabendere et al., "Model-based generation of low distortion currents in grid-coupled pwm-inverters using an LCL output filter," *Power Electronics Specialists Conference, 2004. PESC 04. 2004 IEEE 35th Annual*
[6] T.Wang, Z.Ye et al., "Output filter design for a grid-interconnected three-phase inverter," *Power Electronics Specialist Conference, 2003. PESC '03. 2003 IEEE 34th Annual*
[7] Dahono, P. A., Purwadi, A. e Qamaruzzaman, "An LC Filter Design Method for Single-Phase PWM Inverters," *Proceedings of 1995 International Conference on Power Electronics and Drive Systems. PEDS 95,* v. 2, pp. 571-576.
[8] Col.Wm.T. McLyman, "AC Inductor Design," in *Transformer and Inductor Design Handbook*, 3rd ed., Marcel Dekker, 2004, pp. 10-1–10-13
[9] G.S. Ramana Murthy, "Design of Transformers and Inductors at Power-Frequency –A modified Area-Product method," M.Sc(Engineering) Thesis, Indian Institute of Science, March 1999.